Longitudinal polarization of positrons in ^{22}Na decay

M. Skalsey, T. A. Girard,* and A. Rich
Randall Laboratory of Physics, University of Michigan, Ann Arbor, Michigan 48109
(Received 23 April 1985)

Detailed descriptions are given of previously reported measurements of the longitudinal polarization (P_L) of positrons in the allowed and unique second forbidden weak decays of ^{22}Na. The measurements were performed relative to the allowed decay of ^{68}Ga by application of time-resolved spectroscopy of the $n=1$ hyperfine states of positronium formed in powder media. Assuming the theoretical value $P_L(^{68}\text{Ga})=\beta(0.999\pm0.001)$, the results are $P_L(^{22}\text{Na}, 3^+\rightarrow 2^+)=\beta(+1.003\pm0.011)$ and $P_L(^{22}\text{Na}, 3^+\rightarrow 0^+)=\beta(+1.00\pm0.05)$. The allowed decay result (combined with other ^{22}Na experimental data on the decay rate, the capture ratio, the spectral shape, the $\beta\gamma$ directional correlation, and the weak magnetic form factor) yields a determination of the full weak form factor structure of the transition through second order in recoil. The experimental value for the capture ratio is currently considered to be anomalously low compared to theoretical estimates. Our polarization result is not, however, sufficiently accurate to definitively favor one or the other value. The forbidden decay result, together with model-dependent nuclear structure calculations, restricts the contribution of previously neglected higher-order corrections to the allowed decay to be less than 10^{-8}.

I. INTRODUCTION

The longitudinal polarization (P_L) of beta particles from nuclear decay is an important quantity for studying the electroweak interaction.[1] It is defined as

$$P_L \equiv \langle \boldsymbol{\sigma}\cdot\hat{\mathbf{v}} \rangle = \frac{N_+ - N_-}{N_+ + N_-} , \tag{1}$$

where $\boldsymbol{\sigma}$ are the Pauli spin matrices and N_+ (N_-) are the number of beta particles with spin parallel (antiparallel) to their velocity $\hat{\mathbf{v}}$. Violation of parity in the weak interaction results in the leading-order theoretical prediction for P_L (ignoring nuclear recoil, higher-order forbiddenness, and Coulomb and radiative correction terms) to be

$$P_L = \pm\beta = \pm\frac{|\mathbf{v}|}{c} , \tag{2}$$

where the upper and lower signs refer to positron and electron decays, respectively. This result holds for all allowed and unique forbidden beta decays.

In this article, we present a detailed description of two measurements of the longitudinal polarization of positrons in the allowed ($\Delta J=1$, $\Delta\pi=0$) and unique second forbidden ($\Delta J=3$, $\Delta\pi=0$) transitions of ^{22}Na. Only brief descriptions of the results of these measurements have previously been reported.[1,2] The experiments employed a positron polarimetry technique based on the application of fast coincidence timing spectroscopy to the decay of positronium (Ps) formed in an MgO powder medium situated in a magnetic field of several kilogauss. The polarization results, combined with additional existing experimental data on other decay parameters, permit a determination of all weak form factors describing the allowed decay through second order in recoil.

The motivation for this work arises from the apparent discrepancy between experimental and theoretical electron capture-to-positron emission (ϵ/β^+) ratios in ^{22}Na—a discrepancy which has received extensive attention in recent years.[3,4] Electron exchange and overlap corrections have been shown to have negligible effect on the total capture rate.[5] The ϵ/β^+ disagreement is generally observed in allowed decay as an apparently increasing function of Z.[3] It is thus far without reasonable explanation, and, barring an origin due to, as yet, unaccounted-for systematic effects, may have significant implications in the fundamental understanding of the weak interaction.

In most cases, the decays are pure Gamow-Teller ($\Delta J=\pm1$) transitions, and exhibit normal logft values, thus indicating no unusual reduction in the dominant matrix element.[3] In contrast, the highly hindered, allowed decay of ^{22}Na gives the possibility of significant contributions from second-forbidden and recoil order corrections, which may serve to remove the discrepancy. The analysis, however, requires a complete set of sufficiently accurate data from which to determine the five weak form factors characterizing the allowed decay. In a study by Firestone, McHarris, and Holstein,[5] which included the experimental ft value, the ϵ/β^+ ratio, the spectral shape factor, and the β-γ direction correlation, the results indeed do appear to suggest the presence of larger-than-expected second-forbidden terms. However, these authors are unable to draw any firm conclusions as a result of insufficient and conflicting data and large experimental uncertainties. A subsequent analysis,[6] by Firestone and Harwood, used a value for the "weak magnetism" form factor (one of the five mentioned above) along with the other ^{22}Na data to determine the form factor set. The value of the weak magnetism term was obtained from the measurement of the radiative width of the $M1$ analog gamma ray decay to ^{22}Na via the conserved vector current hypothesis. The additional datum was still inconclusive in resolving the possibly large form factor situation. Although the present measurement fails to remove the difficulties, it does con-

stitute an important addition to the available set of ^{22}Na decay data since a complete form factor set can now be determined without use of the discrepant ϵ/β^+ ratio.

The suggestion of larger-than-anticipated correction terms in the allowed decay is not confined *a priori* to the terms of lowest order (the set of five form factors mentioned earlier). There are other higher-order corrections which have been neglected in theoretical descriptions of the $\beta\gamma$ correlation used in previous analyses. However, the decay of ^{22}Na, shown in Fig. 1,[7] also includes a small branching to the 0^+ ground state of ^{22}Ne via a unique second forbidden β transition. While little is known experimentally about this decay channel, its theoretical description is analogous to a pure Gamow-Teller allowed decay in its domination by a single leading order axial vector matrix element, for which the value of logft (log$ft=13$) is normal for unique second forbidden decay. Thus, deviations of P_L from β are theoretically expected to be of order 10^{-2} to 10^{-3}.

Study of the ^{22}Na unique forbidden decay also serves to establish limits on the neglected higher-order contributions in the allowed decay. This is because the forbidden corrections to allowed decay are formally identical to higher-order corrections to forbidden decay. The only difference between them are the nuclear matrix elements connecting the initial and final states. These matrix elements are similar since the initial state is the same for both transitions. Precise limits on the neglected correction terms for allowed decay are obtained from the forbidden decay since the analogous corrections appear in lower order, but not leading order, in the forbidden decay. While, as in allowed decay, deviations of the spectral shape from theory are not anticipated to appear above the 10^{-2} level, the only previous investigation[8] of a unique decay parameter in ^{22}Na—a spectral shape measurement—although consistent with theory, is sufficiently insensitive to permit deviations of the polarization from β by as much as 15%.

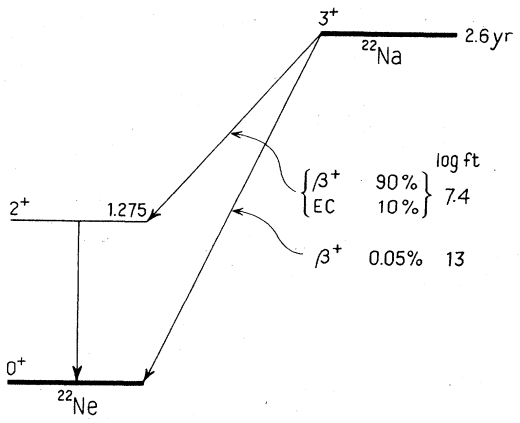

FIG. 1. ^{22}Na decay scheme. The 90% positron feed is an allowed Gamow-Teller transition that is hindered as indicated by log$ft=7.4$. Measurements of the ratio EC/β^+ disagree with theory. The infrequent ground state positron transition is a unique, second-forbidden decay with a normal logft value. The maximum positron energies for the two feeds are 545 and 1830 keV.

As discussed previously,[2] a further motivation for our measurement arises since the shape factor measurements of unique *first* forbidden transitions are generally observed to disagree with theory at the level of several percent. Analysis of these decays in terms of induced correction terms yields contributions which are neither consistent with theory nor internally consistent. The situation is thus far without explanation, and the question of the existence of similar disagreements in higher-order forbidden decay is therefore of some interest.

II. THEORETICAL BACKGROUND

The longitudinal polarization of positrons in the case of pure axial vector (Gamow-Teller) allowed decay is given in general by $P_L=\beta(1+\chi)$, where $\beta=\mathbf{v}/c$ and χ represents recoil order corrections. These corrections, expressed in the elementary particle formalism of Holstein, are, through second order,[9]

$$\chi\simeq\frac{m_e^2}{3M_AE}\frac{1}{c_1^2}\left[c_1(-2c_1+d+2b)-\tfrac{4}{3}M_A(E_0-E)c_1c_2+\frac{3\alpha Z}{4M_AR}c_1h\right], \tag{3}$$

where m_e is the positron rest energy, $E(E_0)$ is the positron total (maximum) energy, R is the nuclear radius in MeV^{-1}, and M_A is the average of parent-daughter nuclear masses. The form factors $\{c,b,d,h\}$ represent the Gamow-Teller, the weak magnetism, the induced tensor, and the induced pseudoscalar contributions, respectively. Only the momentum-transfer (q) dependence of the leading order Gamow-Teller form factor, $c(q^2)\equiv c_1+c_2q^2$, is retained. Modifications to the weak form factor structure of Eq. (3), resulting from Coulomb and radiative effects, are detailed by Holstein[9] and are negligible here.

While compact and relatively transparent, the Holstein formalism[10] is strictly applicable only in allowed decay. In order to accommodate a discussion of the $3^+\rightarrow0^+$ transition, an equivalent multipole expansion formalism[11] is employed from which the polarization deviation from β is generally obtained for the allowed and forbidden ^{22}Na decays as

$$\chi(3^+\rightarrow2^+)=2\frac{\sum_{k_e=1}^{4}\xi_{k_e}\lambda_{k_e}\sum_{L=1}^{3}M_L(k_e,k_\nu)m_L(k_e,k_\nu)}{\sum_{k_e=1}^{4}\Lambda_{k_e}\lambda_{k_e}M_1^2(k_e,k_\nu)} \tag{4a}$$

and

$$\chi(3^+\rightarrow0^+)=2\frac{\sum_{k_e=1}^{4}\xi_{k_e}\lambda_{k_e}M_3(k_e,k_\nu)m_3(k_e,k_\nu)}{\sum_{k_e=1}^{4}\Lambda_{k_e}\lambda_{k_e}M_3^2(k_e,k_\nu)}. \tag{4b}$$

In Eq. (4a), terms with $L\geq4$ are omitted, and M_2^2 and

M_3^2 are neglected relative to M_1^2 in the denominator. For initial (j_α) and final (j_β) nuclear spins, L is constrained by $|j_\alpha - j_\beta| \leq L \leq j_\alpha + j_\beta$, and the sums over k_e are generally terminated beyond $k_e + k_\nu = L + 2$. The quantities ξ_{k_e} are defined as $\xi_{k_e} = \mu_{k_e}\gamma_{k_e}/k_e E$, where $\gamma_{k_e} \equiv [(k_e)^2 - (\alpha Z)^2]^{1/2}$, α is the fine-structure constant, and Z is the atomic number of the daughter nucleus. The μ_{k_e}, λ_{k_e}, and Λ_{k_e} are functions of Coulomb amplitudes, tabulated in Ref. 12. The M_L and m_L represent linear combinations of spin- and energy-dependent functions and the form factor coefficients ${}^{(j)}F_{KLS}^{(n)}$, where $j \equiv (V,A)$, $n = 0,1$. The lengthy expressions for M_L and m_L are well described in the literature,[11,12] and are therefore omitted here. Inclusion of induced corrections is accomplished through modifications of the ${}^{(j)}F_{KLS}^{(n)}$ as described by Buhring and Schulke.[13]

As is evident, the deviations may generally be expressed as a sum of terms in L of the form $\chi \equiv \sum \chi_L$. Aside from denominators, the $L = 3$ contributions to the allowed and forbidden decays differ only in the relative magnitudes of their respective form factor coefficients, and are related by

$$\chi_3(3^+ \to 2^+) = \tfrac{1}{2}\chi_3(3^+ \to 0^+) R_0 R_1 , \tag{5}$$

where

$$R_0 = \frac{\sum_{k_e} \Lambda_{k_e}\lambda_{k_e}[M_3(k_e,k_\nu)]^2_{(3^+\to 0^+)}}{\sum_{k_e} \Lambda_{k_e}\lambda_{k_e}[M_3(k_e,k_\nu)]^2_{(3^+\to 2^+)}} ,$$

$$R_1 = \frac{\sum_{k_e} \xi_{k_e}\lambda_{k_e}[M_3(k_e,k_\nu)m_3(k_e,k_\nu)]_{(3^+\to 2^+)}}{\sum_{k_e} \xi_{k_e}\lambda_{k_e}[M_3(k_e,k_\nu)m_3(k_e,k_\nu)]_{(3^+\to 0^+)}} , \tag{6}$$

such that

$$\sum_{L=1}^{2} \chi_L(3^+ \to 2^+) = \tfrac{1}{2}[\chi(3^+ \to 2^+) - \chi_3(3^+ \to 2^+)] . \tag{7}$$

Thus, to the extent that the ratios of matrix elements can be calculated with certainty, the forbidden decay may be used to further limit the magnitude of the $L = 1,2$ contributions to the allowed decay.

In either formalism, the respective form factors are related to the reduced matrix elements of each transition. The explicit connection is customarily based on the assumption of the impulse approximation, in which off-shell and exchange effects are neglected. For the Holstein form factors, these connections are detailed in Ref. 10. In the case of the form factor coefficients of the multipole expansion formalism, the relations for both allowed and forbidden decays are obtained from general expressions contained in Ref. 13.

The form factors in our work are derived from the reduced matrix elements of Brown and Wildenthal[14] in the form of one-body density matrix elements. The matrix elements are obtained from *sd* shell model wave functions which are determined from effective Hamiltonians (two-body matrix elements and single particle energies), combined with single particle matrix elements. The one-body transition density matrix elements differ from those used in the previous Firestone *et al.* analyses[5] as a result of new, shell model wave functions obtained from a formulation of the effective Hamiltonian which treats the entire *sd* shell.[15] A comparison of new and previous predictions of the allowed decay weak form factor structure is given in Table I, where the associated uncertainties in the new matrix elements are estimated to be of order 20%.[14] For the forbidden decay, the predicted leading order matrix element is consistent with the calculations of Warburton, Garvey, and Towner.[16]

III. EXPERIMENTAL PROCEDURE

The measurements described in this article were performed using a new polarimetry technique based on the time-resolved spectroscopy of magnetically quenched $n = 1$ positronium (Ps). The principle of the technique has been extensively described previously.[17] Briefly, mixing the singlet and $m = 0$ triplet Ps states in an external (polarimeter) magnetic field ($\mathbf{B}_{pol}$) yields a perturbed triplet state which, when created with positrons which have a net polarization on stopping ($\mathbf{P}_{stop}$), has a formation fraction which is a function of $\mathbf{P}_{stop}\cdot\mathbf{B}_{pol}$. Experimentally, the $\mathbf{P}_{stop}\cdot\mathbf{B}_{pol}$ dependence may be observed by either reversing $\mathbf{P}_{stop}$ (inconvenient at beta decay energies) or by reversing $\mathbf{B}_{pol}$ (the technique used here). This reversal gives rise to an asymmetry A, given by:

TABLE I. Shell model estimates of ^{22}Na weak form factor structure.

Weak form factor	FMH[a]	BW[b]	FMH[c]	BW[d]
c_1	+0.002 66	−0.0133	−0.016	−0.016
B	−117	−12.1	+19	−10
C_2	−2.25	−0.154	+0.37	−0.062
D	−19	3.05	+3.2	2.5
H	7.3×10^3	1.2×10^3	-1.2×10^3	9.6×10^2

[a]Firestone, McHarris, and Holstein (Ref. 5).
[b]Brown and Wildenthal (Refs. 14 and 15).
[c]Results of a, normalized to the experimental value of $c_1 = -0.016$ obtained from the logft value (Ref. 5) and sign from Ref. 14.
[d]Results of b, normalized to $c_1 = -0.016$.

$$A=\frac{N_+-N_-}{N_++N_-}\ , \tag{8}$$

where N_+ (N_-) is the number of perturbed triplet Ps atoms formed with $\mathbf{P}_{\rm stop}$ and $\mathbf{B}_{\rm pol}$ antiparallel (parallel). When Ps is formed, the population of the perturbed triplet state (T') will have an asymmetry on B field reversal given by:

$$A_{T'}=P_{\rm stop}\epsilon\cos\theta\ , \tag{9}$$

where $\epsilon=x(1+x^2)^{-1/2}$, $x=0.0276B_{\rm pol}$(kG), and $\cos\theta\equiv-(\hat{\mathbf{P}}_{\rm stop}\cdot\hat{\mathbf{B}}_{\rm pol})$. The lifetime ($\tau_T$) of the unperturbed $m=\pm1$ triplet states (T) does not change from its field-free value of 135 ns in the presence of $\mathbf{B}_{\rm pol}$. The lifetime of the perturbed singlet state (S) is also essentially unchanged from the field-free value of 0.125 ns. However, the $m=0$ (perturbed) triplet state lifetime [$\tau'_T(m=0)$] depends strongly on the magnitude of the perturbing field:

$$\tau'_T(m=0)=\frac{1}{\lambda'_T}=\frac{1+Y^2}{\lambda_T+Y^2\lambda_S}\ , \tag{10}$$

where $Y=x/[1+(1+x^2)^{1/2}]$, and λ_S (λ_T) is the unperturbed singlet (triplet) decay rate. At fields of order 10 kG, $\tau'_T\approx5$–10 ns, permitting separation of T' from the other hyperfine Ps components by the use of fast-timing techniques. The various lifetime components that make up the Ps decay spectrum are displayed in Fig. 2. After 5.5 ns in the decay spectrum all singlet Ps has decayed, all unbound positrons have annihilated and, ignoring the background, the spectrum contains essentially only perturbed and unperturbed triplet Ps. Since only the perturbed state displays the polarization asymmetry and since the lifetimes of perturbed and unperturbed Ps are different, the asymmetry observed in the decay spectrum has a time dependence (time after Ps formation):

$$A(t)=\frac{P\epsilon\cos\theta}{1+\frac{2\lambda}{\lambda'}\exp[(\lambda'-\lambda)t]}\ . \tag{11}$$

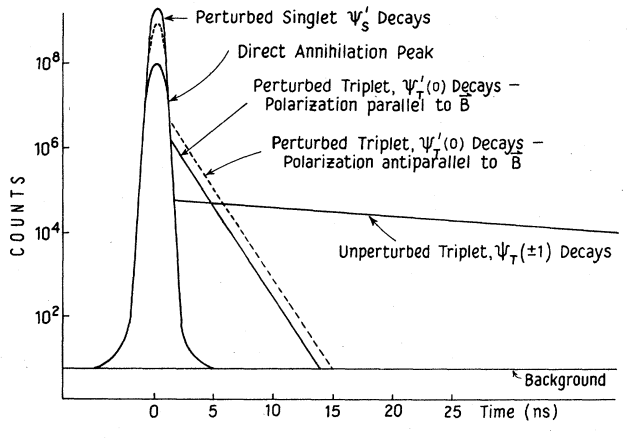

FIG. 2. Time spectrum of $n=1$ Ps decay. The lifetime components in the decay of magnetically-quenched Ps are displayed. The amplitudes of the perturbed triplet and singlet states vary as shown by the broken lines when the polarimeter field direction is reversed.

This formula expresses the fact that the ratio of T to T' events increases with time in the decay spectrum. We measure the total number of events, T and T', in a time window in the decay spectrum (e.g., 5.5 to 30 ns). The asymmetry in the number of events observed in this window, upon field reversal, is related to the polarization by:

$$A=P\epsilon f\ , \tag{12}$$

where f is the fraction of T' events in the time window. The value of f was determined using two independent methods: (1) the spectrum was fitted to a sum of exponentials and the various lifetime components were stripped so that the amplitudes of T,T' and the background could be obtained, and (2) $B_{\rm pol}=0$ measurements were performed, and f was extracted as described in Ref. 18. Both methods yielded $f=0.55\pm0.02$.

Since Ps formation occurs typically at $\simeq$10 eV, the depolarization of initially energetic β decay positrons (energy $\approx$100 keV-1 MeV) constitutes a serious systematic effect (e.g., at 350 keV the uncertainty in polarization is 0.07) for which calculated estimates are accurate to about 50% of the predicted depolarization.[17,19] This difficulty was circumvented in the present experiments by relative measurement between positrons from ^{22}Na and ^{68}Ga. Positrons of equal energy from the two sources were alternately selected for polarization analysis by a β spectrometer, on the assumption that equal-energy positrons depolarize equally on stopping in the polarimeter. The system is shown in Fig. 3.

The polarimeter was constructed from a water-cooled,

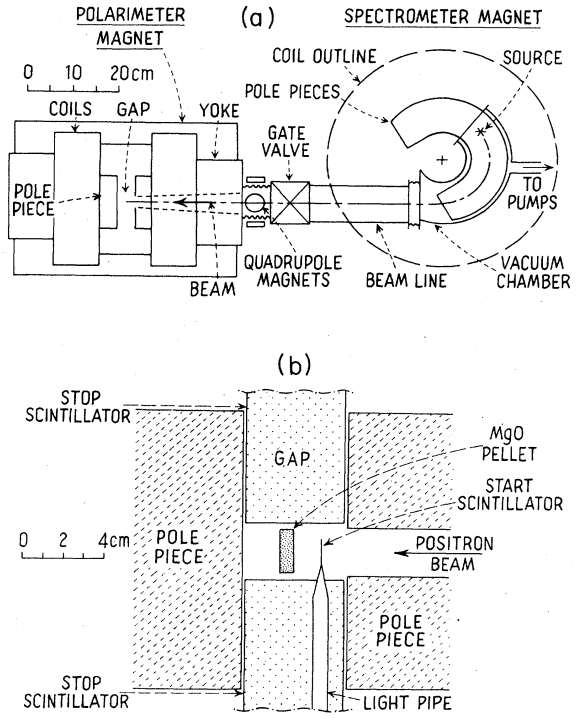

FIG. 3. Spectrometer-polarimeter system. The positron polarization comparator (a sector, β spectrometer coupled to a Ps-based, positron polarimeter) is shown in (a). Detail of the central geometry of the polarimeter is shown in (b).

15.2 cm diam Varian nuclear magnetic resonance (NMR) iron magnet. The positron beam entered the magnet gap parallel to the polarimeter field through a pole piece with a tapered hole drilled along the axis. The gap width of 4.90 cm permitted a maximum magnetic field of 8 kG at the Ps formation site. The Ps formation medium was an extremely fine-grained ($\sim$50 Å) powder of MgO, in which the unperturbed triplet decay rate is essentially unquenched and has been shown to vary by less than 5% from its vacuum value.[17] The powder was obtained from Mallincrodt, and compressed into cylindrical pellet targets of 2.2 cm diam$\times$0.7 cm with a density of 0.3 g/cm^3. Thicker pellets proved necessary in the measurements of the forbidden transition. Each target was heated under vacuum at 350°C for $\sim$4 h in order to remove the decay rate-quenching presence of water vapor, and maintained under a vacuum of 10^{-5} Torr within the polarimeter chamber during measurement.

The decay spectrum was obtained using start-stop timing measurements. The start detector consisted of a 1.27 cm square$\times$0.025 cm thick Pilot *B* plastic scintillator, edge coupled by a lucite light pipe to an RCA 8850 photomultiplier tube located outside both the vacuum system and the magnetic field. The scintillator thickness was chosen to give virtually 100% transmission with 350 keV positrons, the lowest energy used in these studies. The plastic scintillator was positioned within a lead collar 2.22 cm in diameter, which absorbed most of the gamma rays produced by the annihilation of Ps formed by positrons stopped in the thin scintillator. Two stop detectors, forming a disk of Pilot *B* plastic scintillator 4.75 cm thick and 33 cm in diameter, were located outside the vacuum system but within the magnetic field. Each section was coupled by lucite light guides to two RCA 8850 photomultiplier tubes located outside the field. All phototubes were magnetically shielded to prevent gain shifts when the polarimeter field was reversed. The strongest magnetic field at the location of a tube photocathode was 50 G with no shielding, and less than 0.1 G with shielding. No gain-dependent effects from polarimeter field reversal were observed in any of the tubes.

The spectrometer was constructed from an air-cooled mass spectrometer magnet. The pole pieces formed a flat-field *C*-shaped magnet with a gap of 5.1 cm, an average radius of 12.7 cm, and a width of 10.2 cm. The average angle of bend was 125°. The fringing field at the exit plane was used as a focusing element to produce a converging beam with coincident foci, six spectrometer radii from the exit. The primary defining slits were located at 50° (11 cm on the central ray) from the source, and formed a rectangular opening which restricted motion in both the horizontal (5.7 cm) and vertical (1.6 cm) directions. Four additional sets of graphite slits were located downstream from the primary slits but within the spectrometer, and they alternately restricted vertical and horizontal motions.

Four independently-excitable coils were placed in a quadrupole configuration around the beam pipe, as seen in Fig. 3, to compensate for fringing fields from the polarimeter magnet. Independent poles permitted operation as either a singlet quadrupole lens system or a deflection system. The axes of the four coils were positioned at 45° to the horizontal plane, and the maximum magnetic field obtained from a single pole at the center of the beam line was 10 G.

Figure 4 displays the mechanism used to support the sources in the spectrometer and to position alternately each source for polarization analysis. Graphite shields in front of the sources prevented positrons from the source not under investigation from reaching the polarimeter. Externally controlled, adjustable stops for each source provided a range of 1.5 mm for radial positioning. The individual source holders each consisted of a 0.08 mm Mylar tube supporting a single layer ($\sim$40 μg/cm^2) of VYNS (Ref. 20) film 1 cm from an aluminum support ring. A thin layer ($\sim$1 μg/cm^2) of gold was vacuum evaporated onto the VYNS and Mylar to prevent charge buildup.

The ^{22}Na activity was supplied by New England Nuclear Corporation (NEN) in the form of ^{22}NaCl in weak acid solution. A 3 mm$\times$3 mm square of nickel foil (450 μg/cm^2) was placed on the VYNS covering of the source holder, upon which the activity was positioned using the technique of drop deposition and air evaporation, with insulin employed as the wetting agent. A second covering layer of VYNS was then applied to confine the activity. The total thickness of the ^{22}Na source is estimated to be (1.0$\pm$0.2) mg/cm^2, on the basis of the thickness of the Ni backing, the two layers of VYNS, and the actual amount of NaCl deposited. The ^{22}Na supplied by NEN had a specific activity of 306 mCi/mg of Na, and the activity of the source was about 3 mCi. For the measurement of the unique second forbidden decay, a ^{22}Na source of 50 mCi intensity was obtained from NEN. The activity was deposited on a beryllium backing and covered with a 0.005 mm titanium window.

The comparison decay ^{68}Ga was available from NEN as the daughter product of the electron capture decay of ^{68}Ge, and half-life of which is 280 days. The activity was electrocodeposited as $GeCu_3$ onto a small piece (3.0 mm$\times$2.5 mm) of 450 μg/cm^2 nickel foil.[21] After electroplating, the Ni-$GeCu_3$ alloy was attached to the source holder and covered with a layer of VYNS. The primary Ge source used in the polarization studies had an intensity

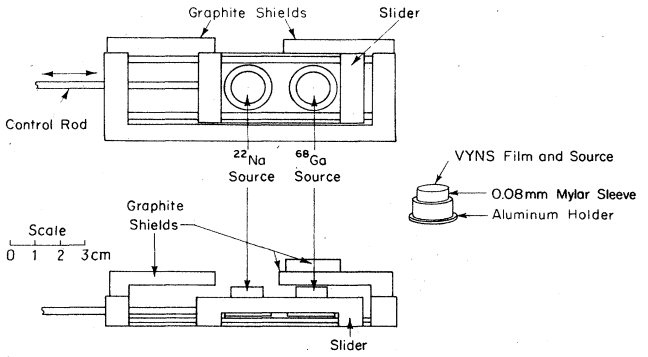

FIG. 4. Source holder and interchange mechanism. Two sources, each in holders shown on the right, are interchanged by a slider operated from the left. One source is used for polarization analysis while the other is shielded.

of 12 mCi, and an estimated thickness of (1.3 ± 0.3) mg/cm^2 based on electroplating tests made with cold Ge and ^{68}Ge tracer. The thicknesses of the test sources were measured using the method of alpha particle energy loss.

The polarimeter electronics are shown in Fig. 5. A Tracor Northern 1710 multichannel analyzer (MCA) accumulated the time spectrum of Ps decay up to 80 ns after $t=0$, a region composed primarily of prompt and perturbed events. Scaler coincidence counters, labeled Bgd and o-Ps, were required to compenstate for gain instabilities in the MCA analog-to-digital converter (ADC—not shown) and the time-to-amplitude converter (TAC). The o-Ps scaler recorded events occurring between 50 and 350 ns after the prompt ($t=0$) events [consisting primarily of unperturbed o-Ps (triplet) decays] and was used as a measure of the total number of Ps atoms formed. The Bgd scaler recorded events 2.4 to 3 μs after $t=0$, allowing the contribution due to background events from uncorrelated start and stop signals to be subtracted. All delay lines and widths were set using coaxial cables to achieve stable operation.

The form of the uncorrelated background (due to start pulses that have no correlated stop pulses, and stop pulses with no correlated starts or where correlated pulses are missed due to background radiation) appearing under the decay spectrum ($t\geq 0$) is, ignoring dead time,

$$\text{Bgd}=B_0\exp(-R_{\text{stop}}t)\ , \tag{13}$$

where t is the time after $t=0$ and R_{stop} is the stop rate at the TAC ($\sim$2 kHz). The background rate at $t=0$, B_0, is given by

$$B_0=(R_{\text{stop}})(R_{\text{start}}^{\text{uncorrel}})\Delta t\ , \tag{14}$$

where $R_{\text{start}}^{\text{uncorrel}}$ is the start rate with no correlated or missed stops and Δt is the time width of the bins in the analyzer spectrum. To eliminate the effects of electronic dead time in the circuit, the "true start" (dead time corrected) output of the TAC was used in both the Bgd and o-Ps coincidence circuits since the TAC has a longer dead time than any other component in the circuit. Uncorrelated start pulses were obtained by inhibiting start pulses which have a correlated stop in the TAC (prompt and perturbed events) or in the o-Ps circuit (unperturbed events). The background corrections had their largest effect in the o-Ps circuit, where typically 3% of the counts

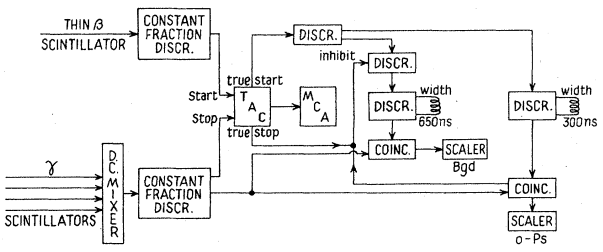

FIG. 5. Polarimeter electronics. Fast-timing electronics are used to process the polarimeter detector outputs. The circuit measures the lifetime decay spectrum of positronium, and permits accurate normalization and background correction.

arose from background events. The Bgd scaler was in operation simultaneously with the o-Ps scaler and the MCA, and ensured that the background correction introduced a maximum uncertainty of 0.2% to the allowed decay polarization comparison.

The comparison of allowed decays was run for 32 days at a positron energy of 350 keV and at an 8 kG polarimeter field, with the data binned into approximately 6 h runs. Either a polarimeter field reversal or a source interchange was alternately affected at the end of each run. The FWHM of the transmission peak at the beam energy was 20 keV, which with the Si detector resolution of 8 keV implies an energy resolution of 18 keV or $\Delta T/T=5.1\%$. Installed in the spectrometer, the average positron energy from each source differed by less than 1 keV. The accuracy with which the source slider reproduces source positions is such that it can cause an observable change in the energy spectra of less than 1 keV for a single source. Reversing the polarimeter field produced a shift of $\sim$2 keV in the location of the centroid of the peak. This shift was the same to within 1 keV for both sources. Since the accuracy in the polarization comparison measurement is determined primarily by the source interchange, rather than the field reversal, this small 2 keV shift has no significant effect on the results. The average start detector rate was 2.6 kHz; the average stop detector rate was 1.9 kHz. The average rate of start-stop coincidences within 80 ns of $t=0$ (TAC rate) was 515 Hz. These rates, corrected for decay, remained stable to within 5% throughout the run.

Measurement of the unique second forbidden decay required a total of six weeks of continuous data acquisition at 800 and 1000 keV using an 8 kG polarimeter field, with data binned into approximately 12 h runs. Either a polarimeter field reversal or source interchange was alternately affected at the end of each run. The noise-corrected start detector rate for ^{22}Na was 55 Hz; the average stop detector rate was 1.7 kHz. The rate of start-stop coincidences within 80 ns of $t=0$ for ^{22}Na was 10 Hz. The ^{68}Ga source used for this comparison was about 0.2 mCi, and gave roughly a six times greater start rate than the ^{22}Na source. The thickness of this ^{68}Ga source was estimated to be 4 mg/cm^2.

IV. DATA ANALYSIS

The decay spectrum of perturbed triplet Ps was observed in 14 time windows, each of 24.5 ns duration with starting times of 5.5, 7.5, 9.5, ... ns after $t=0$. The uncorrelated background contribution to these windows was typically $\sim$0.3% of the counts in a window. The number of events (background corrected) in a perturbed triplet time window, acquired with the polarimeter field alternately antiparallel (N_+) and parallel (N_-) to the β momentum, were normalized to the background-corrected number of unperturbed (N_{oPs}) events, yielding

$$R_\pm=\frac{N_\pm}{N_{\text{oPs}}} \tag{15}$$

so that only Ps events were employed in the analysis. Direct annihilation events (annihilation without Ps forma-

tion, $\tau \approx 0.1$ ns) were excluded by choosing time windows beyond the prompt peak. Most of the previous measurements of polarization using the Ps lifetime technique were normalized to the incident positron rate,[22] and are susceptible to spurious polarization results if the Ps formation fraction changes during measurement. The formation of Ps in MgO allows us to avoid this problem.

The Na-Ga polarization comparison $(\Delta P/P)^{\text{Na-Ga}}$ is determined from the $R_{\pm}$ values by using the relation:

$$\left[\frac{\Delta P}{P}\right]^{\text{Na-Ga}} = (A^{\text{Ga}})^{-1}\frac{\overline{\Delta R}}{\overline{R}} . \tag{16}$$

Here, A^{Ga} is the measured ^{68}Ga asymmetry and

$$\overline{\Delta R} = R_{+}^{\text{Na}} - R_{+}^{\text{Ga}} = R_{-}^{\text{Ga}} - R_{-}^{\text{Na}} ;$$

$$2\overline{R} = R_{+}^{\text{Ga}} + R_{-}^{\text{Ga}} = R_{+}^{\text{Na}} + R_{-}^{\text{Na}} .$$

The observed polarization comparison curve (as a function of the 14 sequential perturbed time windows) is then expected to arise from Ps in MgO (10 ns lifetime) which dominates at long times, and a "plastic scintillator" component (2 ns lifetime) which dominates at short times (see Fig. 6). This "scintillator" component is due to positrons that form Ps in the plastic. A major fraction (85—90%) of these positrons backscattered from the MgO pellet before stopping in the plastic. Only 10—15% of the plastic component is due to beam positrons that are stopped directly in the start scintillator. In the first time window in Fig. 6(a) there is 12σ disagreement between values of $(\Delta P/P)^{\text{Na-Ga}}$ for the field alternately parallel and antiparallel to the positron momentum. Specifically, we find $(\Delta P/P) = -18.6(8)\%$ for B parallel and $(\Delta P/P) = -5.0(8)\%$ for B antiparallel. The cause of the effect is probably due to the slightly different spatial distributions of the two sources. A difference in the location of the beam incident on the start detector results in a difference in the detection efficiency of the stop detector. The difference in the number of 2 ns decays that would be detected due to the location difference could result in the observed shape in the polarization curve. However, the size of the observed effect is an order of magnitude larger than expected from an estimate of the expected variation of 2 ns decay detection efficiency.

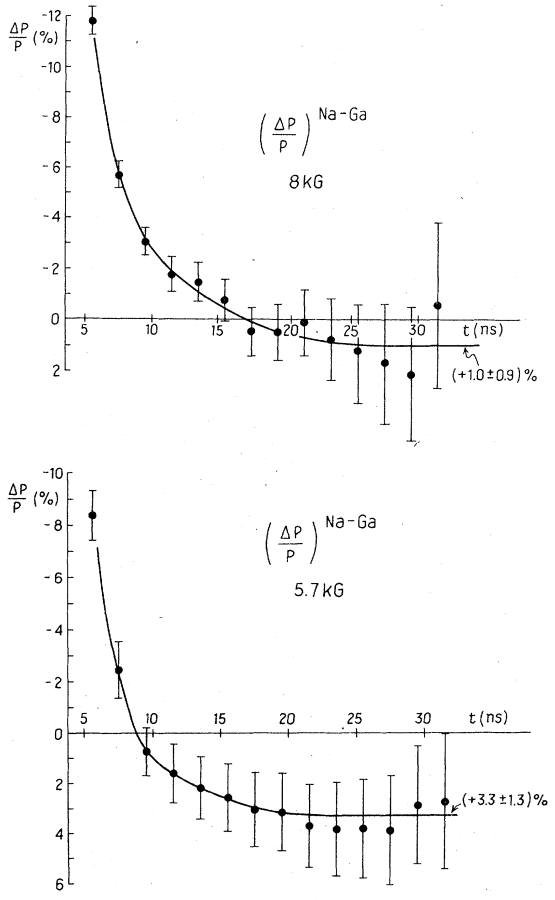

FIG. 6. Polarization comparison data. The results of the Na/Ga polarization comparison at (a) 350 keV and 8 kG and (b) at 350 keV and 5.7 kG, as a function of the starting time of the perturbed window. Contamination from 2 ns Ps formed in the plastic scintillator is clearly present in the early time windows. Error bars shown are correlated since the windows overlap.

The presence of the large, anomalous polarization effect in the early time window necessitated analyzing the results of the polarization comparison as a function of perturbed window starting time. The assumption was made that early time windows are contaminated by the 2 ns Ps component. Without the presence of the 2 ns component, the polarization comparison result would be independent of the perturbed window chosen, and is referred to as the "asymptotic value" since at long times the curve approaches a straight, horizontal line [+1.0% in Fig. 6(a) and +3.3% in Fig. 6(b)].

V. SYSTEMATIC EFFECTS AND CORRECTIONS

The allowed decay measurement was repeated at polarimeter magnetic fields of 6.5 and 5.7 kG, followed by a comparison at 400 keV and 8 kG. These additional comparisons were performed to explore energy-dependent systematic effects (which are likely to be small, since scattering effects at 400 keV are not appreciably different from those at 350 keV) and to check the effect of the higher efficiency of 400 keV positrons for penetrating the start detector. The comparisons were also used to search for systematic effects dependent on the polarimeter field. Such effects seemed more likely than the energy dependent effects since field changes influence a number of possibly significant parameters. For example, the field gradient at the polarimeter entrance depends on $|B_{\text{pol}}|$, so that positrons deflected by this gradient into helical trajectories experience a field-dependent depolarization (discussed further at the end of this section).

Field- and energy-dependent systematic effects were found to be small, as is evident from the experimental polarization results. Table II displays the asymptotic values found from the 14 perturbed windows, as shown in Fig. 6, and the weighted average of the four allowed decay runs. The 2.5% error in the 400 keV run is not used in assessing the error in the average since the likelihood of energy-

TABLE II. Polarization comparison results.

B_{pol}	$E_{\beta+}$	$(\Delta P/P)^{Na\text{-}Ga}$	
		Allowed decay	
8 kG	350 keV	(+1.0±0.9)%	
6.5 kG	350 keV	(+0.7±1.4)%	(+2.1±0.95)%
5.7 kG	350 keV	(+3.3±1.3)%	
8 kG	400 keV	(+2.5±2.5)%	
average		(+1.5±0.95)%	
		$\chi^2=2.71$ for three degrees of freedom	
		Forbidden decay	
8 kG	800 keV	(−5±5)%	
8 kG	1 MeV	(+3±5)%	
average		(−1±5)%	

dependent systematic effects is considered small. Polarimeter field-dependent systematic effects are more likely, and consequently, the errors in the low field runs were used to arrive at the quoted error for the average value. First, we averaged together the results of the two low field runs (5.7 and 6.5 kG) obtaining $(\Delta P/P)^{Na\text{-}Ga}=(+2.1\pm0.95)\%$, as shown in Table II. This value agrees well with the result of the 8 kG run $[(\Delta P/P)^{Na\text{-}Ga}=(+1.0\pm0.9)\%]$. Averaging of these two quantities is clearly justified, but reducing the error is not since field-dependent systematic effects are likely. The apparent absence of field-dependent effects in these data implies a reliable result for the average at the error quoted (0.95%), and not at the 0.6% level obtained by simply combining the errors.

Other known systematic effects are separated into two classes, depending upon their association with either the spectrometer or polarimeter operation. Most of the polarimeter related effects have their origin in the electronic circuit used to measure Ps lifetimes. For a TAC range of 100 ns, shifts in the apparent time location for prompt events of order 5 ps over 15 min periods were measured. Binning the data into approximately 100 separate runs introduced an uncertainty of 0.15% in the polarization measurement due to time shifts. With a TAC range of 2 μs, shifts of about 100 ps were measured. These shifts were consistent with the gain stability specifications of the TAC and ADC in the MCA.

Count rate dependent systematic effects were investigated in a polarization comparison performed using two ^{68}Ga sources whose intensities differed by a factor of 12. No difference in the measured polarization was found at the level of 1.7%. In the polarization comparison of allowed ^{22}Na and ^{68}Ga decays, the rates were the same to within 25% for the two sources. Assuming a linear relation between rate difference and $\Delta P/P$, count rate dependent effects were excluded at the level of 4×10^{-4} in this comparison.

The temperature dependence of the propagation time for a timing pulse in RG-58 coaxial cable was found to be −150 ppm/°C, that is, the warmer cable causes faster pulse propagation. The cables most sensitive to this effect are the start and stop cables leading to the TAC, with a difference in length of 17 ns. A random 1 °C shift in temperature, when averaged over the 100 separate runs, results in a statistical spread in the polarization comparison of 8×10^{-4}.

All spectrometer-related systematic effects arise from the scattering of positrons from various surfaces, including the sources themselves. The differential depolarization of positrons scattered in the sources was calculated using the theoretical expressions of Muhlschlegel,[23] which include the effects of (1) large angle single scatterings and (2) small angle multiple scattering. The results for 350 keV positrons are shown in Table III, with the predicted source depolarization decreasing rapidly with increasing energy, as does the ratio of multiple/single scattering effects.

The assumption that systematic effects due to scattering from surfaces in the spectrometer will cancel between the two sources in the polarization comparison is not generally justified, since most of the ^{68}Ga positron distribution lies above 350 keV, while most of the allowed ^{22}Na distribution lies below. Thus, differential scattering effects are expected to be severe. A Monte-Carlo study of scattering in the spectrometer[24] was performed to provide (1) an estimate of the magnitude of the scattering from the various surfaces and (2) the energy distribution of the scattered particles that reach the polarimeter after the scattering has occurred. The latter is important to the measurement of scattering contributions, since the program identifies regions in the energy spectrum in which particles that have scattered from a given surface are likely to appear.

Five scattering surfaces in the spectrometer were investigated. As anticipated, the contribution of scattering

TABLE III. Systematic effects. Systematic uncertainties in the allowed decay polarization comparison are individually displayed. See Table I of Ref. 2 for the systematic uncertainties in forbidden decay results.

Systematic	Effect ($\times 10^{+2}$) $\epsilon(^{68}Ga)^a$	$\epsilon(^{22}Na)^a$	Δ(Ga-Na)
Spectrometer:			
Source depolarization	-0.49 ± 0.35	-0.26 ± 0.20	-0.23 ± 0.23
Source alignment			0.00 ± 0.06
Scattering:			
source holder	-0.50 ± 0.19	-0.05 ± 0.05	-0.45 ± 0.20
first slit	-0.09 ± 0.09	-0.02 ± 0.02	-0.07 ± 0.09
vacuum chamber	-0.24 ± 0.12	-0.03 ± 0.03	-0.21 ± 0.12
shield	-0.23 ± 0.31	-0.03 ± 0.03	-0.20 ± 0.31
back scattering	-0.03 ± 0.06	-0.01 ± 0.01	-0.02 ± 0.06
Shield leakage	0	-0.05 ± 0.05	$+0.05\pm0.05$
Polarimeter:			
Time shifts			0.00 ± 0.15
Dead time, background			0.00 ± 0.20
Temperature of cable			0.00 ± 0.08
Count rate			0.00 ± 0.04
Net Effect			$(-1.13\pm0.54)\%$

[a] ϵ is the fractional depolarization. When $P_i=\beta$, depolarization results in $P_f=\beta(1+\epsilon)$.

from the aluminum source holder and slider mechanism was the largest systematic effect identified. This contribution was measured by replacing the start detector with a Si surface barrier detector and masking the aluminum source holder with a lead foil collar. The change in rate of the arrival of positrons at the polarimeter with and without the Pb collar was assumed to be due to the change in the number of positrons scattered from the holder. Using tabulated back scattering coefficients,[25] the change in rate was related to the number of positrons that scatter from the holder and the depolarizing effect extracted.

Scattering from the graphite shields was investigated in a similar manner. Energy spectra were taken with and without lead foil covering the shields, and the observed rate difference was related to the scattering of positrons from this surface. The backscattering of positrons from the vacuum flange located behind the sources was reduced by a layer of graphite placed on its inside surface. The backscattering contribution from the graphite was investigated by placing lead foil over the graphite flange, as in previous studies, to increase the scattering. Additionally, a small graphite plug was fashioned to fit 1 cm behind the source (instead of 3.75 cm to the flange). By inserting the plug and measuring the change in rate, the backscattering contribution was again determined. Finally, a polarization comparison was performed on a ^{68}Ga source with and without the plug inserted, yielding the result $(-1.5\pm1.5)\%$. As shown in Table III, tests indicated that backscattering contributed less than 10^{-3} uncertainty to the comparison.

The scattering of positrons from the first defining slit is also a possible source of systematic error. Space and access restrictions in the spectrometer vacuum chamber made it impossible, experimentally, to investigate scattering from these surfaces as was discussed above for the other surfaces. Using the size of the scattering systematics from the holder and the shield studies as a basis, an estimate was made (as appears in Table III) of the size of the slit scattering effect with primary consideration for geometric effects. The Monte-Carlo program, however, predicts this effect to be two orders of magnitude smaller than shown, so that the estimate presented should then be taken as a conservative upper limit.

Scattering from the "vacuum chamber" describes events in which the positron, after scattering, experiences little or no energy selection by the spectrometer. These scatterings occur in the region beyond the first defining slit, and are indicated by an event registered in the Si detector at an energy above the beam energy. Approximately 2.7% of the events in the spectrum lie in this region, the majority of which are due to summing of positron kinetic energy and annihilation gamma ray energy. Additionally, two 10.2×10.2 cm diam NaI(Tl) detectors were positioned outside the vacuum chamber 30.5 cm from the Si detector and 180° from each other, and a fivefold coincidence required to record a Si detector signal, i.e., a triple-time coincidence of all three detectors registering events, with each NaI detector required to have 511 keV of energy deposited. The latter constraint ensured that an annihilation gamma ray did not interact with the Si detector in events which passed these cuts. With the possibility of signal summing removed, over 90% of the

high energy events in the energy spectra disappeared, and the depolarizing effect of the remainder is shown in Table III.

The final systematic effect to be discussed here is the positron depolarization that occurs in traversing the polarimeter field gradient. As noted earlier, several polarization runs at different fields (see Table II) indicate that this effect is at or below the 1% level. To further strengthen this claim, absolute polarization measurements were performed at 350 keV resulting in

$$P_L(^{68}\mathrm{Ga})=(+0.89\pm0.09\pm0.02)\beta$$

and (17)

$$P_L(^{22}\mathrm{Na})=(+0.88\pm0.09\pm0.03)\beta\ ,$$

where the first error is due to uncertainty in the calculation of stopping depolarization and the second error is due to all other systematic and statistical uncertainties. If we ignore the first error and assume that the depolarization calculation is correct, a depolarization of approximately 12% is apparent. However, there is an equal effect on each source, so that the error due to depolarization on entering the magnet is canceled in the polarization comparison. Therefore, the absolute measurements, taken together with the polarimeter field variation data in Table II, indicate the reliability of the polarization comparison technique at the 1% level.

VI. RESULTS AND DISCUSSION

Combining systematic and statistical uncertainties, the final results for the polarization comparison of ^{22}Na and ^{68}Ga are

$$\frac{\Delta P}{P}(\text{allowed})=0.004\pm0.011\ ,$$
$$\frac{\Delta P}{P}(\text{forbidden})=0.00\pm0.05\ . \tag{18a}$$

Assuming[9,10,26] $P_L(^{68}\mathrm{Ga})=\beta(0.9987\pm0.0013)$, we find the longitudinal polarization of positrons in the two feeds of ^{22}Na to be

$$P_L(3^+\to2^+)=\beta(+1.003\pm0.011)\ ,$$
$$P_L(3^+\to0^+)=\beta(+1.00\pm0.05)\ . \tag{18b}$$

The allowed $3^+\to2^+$ result constituted, when first published,[1] an order of magnitude improvement in the determination of positron polarization.[17,22,27] We note for completeness that recently a positron polarization comparison result which employed Bhabha scattering on the nuclei $^{26}\mathrm{Al}^m$ and ^{30}P and which was accurate to 3.8% has been published.[28] The Bhabha technique has the advantage of being usable with positrons of energy greater than 2 MeV, at which energy the depolarization using our technique is approximately 50% thus reducing the utility of the Ps technique at these high energies. Disadvantages of the Bhabha polarimeter are its low efficiency and low asymmetry as compared to the Ps polarimeter; features which make it less useful for most e^+ polarization measurements.

In the case of the forbidden decay measurement, the result is consistent with theory in leading order and further restricts by a factor of 3 the possible existence of any large polarization deviation from β as is now permitted by the spectral shape data. Nevertheless, there remains considerable room for accommodating the anomalous corrections implied by analyses of the first forbidden decay data. Use of Eq. (5) together with model-calculated form factor coefficient ratios, yields

$$\chi_3(3^+\to2^+)\leq2.5\times10^{-8} \tag{19}$$

which is consistent with order of magnitude estimates obtained from theory.[11] This suggests that there are no unusually large contributions to the allowed decay from the previously-neglected correction terms beyond $L=2$.

In principle, the measurement of the allowed decay polarization, in combination with previous measurements of the ft value, the ϵ/β^+ ratio, the spectral shape factor, and the β^+-γ directional correlation forms a complete set of experiments from which all form factors describing the decay through second order in recoil may be derived. Measurements of the beta-gamma circular polarization (CP) correlation β-γ_{CP} have also been performed using ^{22}Na decay,[29] but these results are not considered here due to the large experimental error reported for them. The situation regarding the additional experimental decay data is reviewed in detail by Firestone *et al.*,[5] from whom we adopt the values: $\log ft=7.42$, spectral shape factor $(S)=(0.05\pm0.17)\times10^{-2}$ MeV^{-1}, skew ratio $=0.92\pm0.02$ [the skew ratio R is defined as $R\equiv(\epsilon/\beta)/(\epsilon/\beta)_0$, where $(\epsilon/\beta)_0$ is the theoretical ratio without exchange or overlap corrections], and $\beta\gamma$ directional correlation coefficient $(A_{22})=(-1.2\pm0.5)\times10^{-3}$. The value adopted for A_{22} represents the average of two measurements,[30] which disagree by 2.4 standard deviations, and suggest some caution in the interpretation of the derived results.

The theoretical descriptions of these observables in the Holstein formalism have been given previously:[5]

$$R\approx1-(-1.56B-0.70D+0.0013H+18.0C_2)\times10^{-3}\ ; \tag{20}$$
$$S\approx-(1.79B-0.17D+0.000\,74H-7.78C_2)\times10^{-3}\ \mathrm{MeV}^{-1}\ ; \tag{21}$$
$$A_{22}\approx(4.4B+4.4D-0.60C_2)\times10^{-5}\ ; \tag{22}$$

where the form factors have been redefined as $B\equiv b/Ac_1$, $C_2\equiv c_2/R^2c_1$, $D\equiv d/Ac_1$, and $H\equiv h/A^2c_1$. The Gamow-Teller form factor is obtained as $|c_1|=0.016$ from the decay ft value, neglecting correction terms which are estimated to change c_1 by only a few percent.[5] The weak magnetism form factor is obtained as $B=-14\pm4$ from the radiative width of the analog $M1$ transition.[6] This value assumes no $E2$ admixture to the

$M1$ decay, which would tend to decrease the result. Equations (20)—(22) do not include higher-order quadratic radiative effects. Also neglected, on the basis of shell model estimates coupled with kinematic contributions, are the additional form factors f, j_1, and j_2, present in the general expansion of A_{22}. To the extent that the above model-dependent analysis of the forbidden decay polarization measurement can be accepted, this neglect is clearly justified. In this notation, $P_L(3^+ \rightarrow 2^+)$ at $E = 861$ keV is

$$\beta^{-1}P_L \simeq 1 - 10^{-4}(2.16B + 1.08D + 0.0038H - 0.08C_2) . \quad (23)$$

Simultaneous solution of Eqs. (21)—(23) with the adopted experimental results yields

$$C_2 = -2.8 \pm 1.2 ,$$
$$D = -14 \pm 12 , \quad (24)$$
$$H = (0.4 \pm 2.9) \times 10^4 ,$$

which, together with $B = -14 \pm 4$, constitutes the best estimate to date of the ^{22}Na weak form factor structure obtained solely from experimental data. This structure is compared with the calculated shell model estimates in Table IV (Analysis 1). As is evident, while continuing to suggest larger than anticipated decay corrections, the results presented in Eq. (24) lack sufficient accuracy to be useful in assessing the expected level of contribution to the various observables since, with the exception of B, all are consistent with zero.

Substitution of Eq. (24) into Eq. (20) yields $R - 1 = (2.4 \pm 4.5) \times 10^{-2}$, which is consistent with experiment at the 2σ level [recall $(R-1)_{\text{expt}} = (-8 \pm 2) \times 10^{-2}$]. An analysis in which S is replaced with R yields a virtually identical form factor structure except that $C_2 > 0$ (see Table IV, Analysis 2).[31] Using over-specified analyses employing *both* S and R (and excluding either P_L or A_{22}), we are unable to generate a real solution as a result of the difference in the sign of C_2. Thus, the uncertainties in the form factor determinations are too large to permit definite conclusions.[32]

As indicated in Ref. 5, the error estimates in the measurement of S may be overly optimistic as a result of neglected experimental corrections arising from photon emission, annihilation in flight, and escape of positrons from the detector crystal. Use of the suggested corrected value [$S = (5.9 \pm 3.0)\%/\text{MeV}$], however, yields form factors which are only marginally different in value from those listed in Eq. (24) (see Table IV, Analysis 1'), and this analysis provides no resolution of the above difficulties in analyses involving both S and R.

VII. CONCLUSIONS

The longitudinal polarization of positrons in the allowed and forbidden decays of ^{22}Na have been measured, relative to ^{68}Ga, to accuracies of 1% and 5%, respectively. The measurements were carried out using a new technique in positron polarimetry based on Ps time spectroscopy. The forbidden decay measurement is the first beta polarization determination in second-forbidden unique decay.[2] The allowed decay measurement is the most accurate positron polarization measurement extant and is in fact comparable to the best electron polarization measurements[33] using Mott scattering. It is anticipated that a straightforward redesign of our instrument incorporating higher fields, higher transmission, and better time resolution should result in an order of magnitude improvement in the precision that can be achieved. We have detailed in Ref. 1 plans to apply a redesigned instrument to a new, high precision, on-line experiment. That experiment is presently underway.

The situation regarding model-independent knowledge of the weak form factor structure of the allowed ^{22}Na decay remains unsatisfactory. The present analysis yields correction terms through second order in recoil which are consistent with impulse approximation estimates and the anomalous ϵ/β^+ ratio. However, the allowed decay polarization result is not of sufficient precision to confirm or refute the anomalous ϵ/β^+ measurements. An order of magnitude improvement in the present measurement (from 1.1% to 10^{-3}) is perhaps feasible in a relative measurement employing either ^{64}Cu or ^{58}Co as the normalizing decay with ^{22}Na since spectrometer-associated scattering systematics are virtually eliminated by the near-equality of the comparison β distributions. Improved accuracy in the polarization measurement alone, however, will not resolve the ϵ/β^+ problem. The experimental precision of the β-γ directional correlation, A_{22}, must also be improved by an order of magnitude for a decisive test of the ϵ/β^+ anomaly.

The forbidden decay measurement, the first such measurement of its kind, in combination with model-

TABLE IV. Experiment-based ^{22}Na weak form factor determinations.

Form factor	Theory (SPSM)[d]	Experiment Analysis 1[a]	Analysis 1'[b]	Analysis 2[c]
B	-10	$-14(4)$	$-14(4)$	$-14(4)$
C_2	-0.062	$-2.8(1.2)$	5.3(1.2)	2.5(2.2)
D	2.5	$-14(12)$	$-13(12)$	$-13(12)$
H	9.6×10^2	$3.9(29) \times 10^3$	$3.7(29) \times 10^3$	$3.8(29) \times 10^3$

[a]Analysis 1 using data set $\{B, P_L, A_{22}, S\}$.
[b]Analysis 1' using same data set as 1, but with Firestone-suggested (Refs. 5 and 6) correction of S.
[c]Analysis 2 using data set $\{B, P_L, A_{22}, R\}$, gives $S = 4\%$.
[d]Single particle shell model estimate, normalized to $c_1 = -0.016$ (see Table I).

dependent nuclear structure calculations, restricts the contributions of higher-order recoil corrections to the allowed transition to be less than 10^{-8}. However, our accuracy is still not sufficient to resolve any questions of interest regarding unique forbidden decay. We anticipate that it should be possible to improve the statistical efficiency of the positron polarization comparator (PPC) and reduce its differential source depolarization so that reduction of uncertainty by a factor of 3—4, i.e., to the 1% level will be feasible. However, precision measurements of order 10^{-3}, required to provide critical testing of the decay structure, cannot be realistically envisioned at present. As noted previously,[2] the same technique applied to ^{84}Rb decay suggests the possibility of an eventual 0.5% experimental accuracy. Such accuracy would be useful in directly exploring the question raised by unique first forbidden transitions.

ACKNOWLEDGMENTS

We acknowledge useful discussions with J. Bardwick, R. Firestone, D. Gidley, H. Griffin, M. Hatamian, B. Holstein, J. Van Klinken, D. Newman, D. Paul, A. Vander Molen, and H. Wildenthal. One of us (T.A.G.) further acknowledges useful conversations with B. A. Brown and P. Lipnik during various phases of the form factor analyses. This work was supported by Department of Energy (DOE) grant DOE-C-79ER10451, by NSF grants PHY-8305749 and by PHY-8403817, and by a grant from the Office of the Vice President for Research of the University of Michigan.

*Present address: Institute de Physique, Universite de Louvain, Louvain-la-Neuve, Belgium B-1348.

[1]M. Skalsey, T. A. Girard, D. Newman, and A. Rich, Phys. Rev. Lett. **49**, 708 (1982); M. Skalsey, T. A. Girard, D. E. Newman, and A. Rich, Bull. Am. Phys. Soc. **26**, 1126 (1981); **26**, 1114 (1981).

[2]M. Skalsey, T. A. Girard, and A. Rich, Phys. Rev. C **28**, 1752 (1983); T. A. Girard, M. Skalsey, and A. Rich, Bull. Am. Phys. Soc. **27**, 697 (1982).

[3]W. Bambynek, H. Behrens, M. H. Chen, B. Crasemann, M. L. Fitzpatrick, K. W. D. Ledingham, H. Genz, M. Mutterer, and R. L. Intemann, Rev. Mod. Phys. **49**, 77 (1977).

[4]B. R. Holstein, Phys. Rev. C **15**, 2253 (1977); **20**, 387 (1979).

[5]R. B. Firestone, Wm. C. McHarris, and B. R. Holstein, Phys. Rev. C **18**, 2719 (1978).

[6]R. B. Firestone and L. H. Harwood, University of California Lawrence Berkeley Laboratory Report LBL-12219 (unpublished).

[7]C. M. Lederer *et al.*, *Table of Isotopes*, 7th ed. (Wiley, New York, 1978).

[8]B. T. Wright, Phys. Rev. **90**, 159 (1953).

[9]B. R. Holstein, Phys. Rev. C **16**, 1258 (1977); T. A. Girard, *ibid.* C **27**, 2418 (1983).

[10]B. R. Holstein, Rev. Mod. Phys. **46**, 789 (1974).

[11]H. Behrens and W. Buhring, Nucl. Phys. **A162**, 111 (1971).

[12]H. Behrens and J. Janecke, in *Numerical Tables for Beta Decay and Electron Capture, Landholt-Bornstein, New Series,* edited by K. H. Hellwege (Springer, New York, 1969).

[13]W. Buhring and L. Schulke, Nucl. Phys. **65**, 369 (1965).

[14]B. A. Brown and B. H. Wildenthal, private communication.

[15]B. A. Brown and B. H. Wildenthal, Phys. Rev. C **27**, 1296 (1983).

[16]E. K. Warburton, G. T. Garvey, and I. S. Towner, Ann. Phys. (N.Y.) **57**, 174 (1970).

[17]A. Rich, Rev. Mod. Phys. **53**, 127 (1981); G. Gerber, D. Newman, A. Rich, and E. Sweetman, Phys. Rev. D **15**, 1189 (1977).

[18]P. W. Zitzewitz, J. C. Van House, A. Rich, and D. W. Gidley, Phys. Rev. Lett. **43**, 1281 (1979).

[19]C. Bouchiat and J. M. Levy-LeBlond, Nuovo Cimento **33**, 193 (1964); C. K. Iddings, G. L. Shaw, and Y. S. Tsai, Phys. Rev. **135**, B1388 (1964).

[20]D. Green, J. Sci. Instrum. **38**, 333 (1961).

[21]T. A. Girard, M. Skalsey, E. Sweetman, D. E. Newman, and A. Vander Molen, Nucl. Instrum. Methods **205**, 567 (1983).

[22]A. Bisi, A. Fiorentini, E. Gatti, and L. Zappa, Phys. Rev. **128**, 2195 (1962); L. Dick, L. Feuvrais, and M. Spighel, Phys. Lett. **7**, 150 (1963); J. R. Gilleland and A. Rich, Phys. Rev. A **5**, 38 (1972).

[23]B. Muhlschlegel, Z. Phys. **155**, 69 (1959).

[24]M. S. Hatamian, T. A. Girard, and M. Skalsey, Nucl. Instrum. Methods **222**, 548 (1984).

[25]T. Baltakmens, Nucl. Instrum. Methods **125**, 169 (1975); I. K. MacKenzie, C. W. Schulte, T. Jackman, and J. L. Campbell, Phys. Rev. A **7**, 135 (1973); H. H. Seliger, Phys. Rev. **88**, 408 (1952).

[26]B. R. Holstein, private communication.

[27]L. A. Page and M. Heinberg, Phys. Rev. **106**, 1220 (1957).

[28]J. Van Klinken *et al.*, Phys. Rev. Lett. **50**, 94 (1983).

[29]H. Schopper, H. Behrens, H. Muller, J. Gorres, W. Jungst, and H. Appel, Nucl. Instrum. Methods **49**, 277 (1967); O. Mehling and H. Daniel, Nucl. Phys. **A124**, 320 (1969).

[30]R. M. Steffen, Phys. Rev. Lett. **3**, 277 (1959); H. Muller, Nucl. Phys. **74**, 449 (1965).

[31]While the impulse approximation estimates require C_2 and H to be of opposite sign, such estimates may be unreliable in the calculation of C_2 in hindered decay (see E. E. Saperstein and M. A. Troitskii, Yad. Fiz. **22**, 257 (1975) [Sov. J. Nucl. Phys. **22**, 132 (1976)] and Ref. 5). Moreover, C_2 scales linearly with H in accordance with the partially-conserved axial current (PCAC) hypothesis (Ref. 10).

[32]The situation is further confused by the neglect of potentially-large meson exchange corrections to D [see K. Kubodera, J. Delorme, and M. Rho, Nucl. Phys. **B66**, 253 (1973)]. The magnitude of these corrections is related to the C_2 form factor.

[33]J. Van Klinken, Nucl. Phys. **75**, 145 (1966); A. R. Brosi, A. I. Galonsky, B. H. Kelelle, and H. B. Willard, *ibid.* **33**, 353 (1962); H. Wenninger, J. Stiewe, H. Muusz, and H. Leutz, *ibid.* **A96**, 177 (1967).